PHYSICAL REVIEW B **82**, 165451 (2010)

Molecular self-organization: Predicting the pattern diversity and lowest energy state of competing ordering motifs

B. A. Hermann,[1,*] C. Rohr,[1] M. Balbás Gambra,[2] A. Malecki,[1] M. S. Malarek,[3] E. Frey,[2] and T. Franosch[4,2]

[1]*Center for Nano Science (CeNS) and Walther-Meissner-Institute of Low Temperature Research of the Bavarian Academy of Sciences, Walther-Meissner-Str. 8, 85748 Garching, Germany*

[2]*Arnold Sommerfeld Center for Theoretical Physics (ASC) and Center for Nano Science (CeNS), Department of Physics, LMU München, Theresienstraße 37, 80333 München, Germany*

[3]*Department of Chemistry, University of Basel, Spitalstrasse 51, 4056 Basel, Switzerland*

[4]*Institut für Theoretische Physik, Universität Erlangen–Nürnberg, Staudtstraße 7, 91058 Erlangen, Germany*

(Received 22 March 2010; revised manuscript received 12 May 2010; published 29 October 2010)

Self-organized monolayers of highly flexible Fréchet dendrons were deposited on graphite surfaces by solution casting. Scanning tunneling microscopy (STM) reveals an unprecedented variety of patterns with up to seven stable hierarchical ordering motifs allowing us to use these molecules as a versatile model system. The essential molecular properties determined by molecular mechanics simulations are condensed to a coarse grained interaction-site model of various chain configurations. In a Monte Carlo approach with random starting configurations, the experimental pattern diversity can be reproduced in all facets of the local and global ordering. Based on an energy analysis of the Monte Carlo and molecular mechanics modeling, the thermodynamically most stable pattern is predicted and shown to coincide with the pattern which dominates the STM images after several hours or upon moderate heating.

DOI: 10.1103/PhysRevB.82.165451 PACS number(s): 68.43.−h, 68.37.Ef, 81.16.−c

I. INTRODUCTION

Organic molecules mainly self-organize via hydrogen bonds,[1,2] metal-coordination,[3] or van der Waals interactions.[4] The need has been established for[5,6] more innovative modeling approaches[7,8] that can analyze and predict molecular patterns, thus nurturing efficient application in surface functionalization,[9] sensors,[10] catalysis,[11] and molecular electronic devices.[12] Predictability of surface patterning could speed up molecular design and advance the understanding of the self-organization process itself. For *predicting* several coexisting ordering motifs (cf. Refs. 13 and 14) a new multimodeling approach is required, that does not rely on the prior knowledge of the resulting patterns.[15–19] In this paper we demonstrate that, based on a coarse grained interaction-site model (omitting chemical details), we are able to not only reproduce and predict all features of the local and global ordering motifs of self-organized molecular layers, but also, independently predict the thermodynamically most stable patterns and thus deliver an innovative method for understanding molecular self-organization.

In this paper, the self-organization of flexible supramolecular building blocks, Fréchet dendrons,[20,21] is investigated in highly resolved scanning tunneling micrographs and modeled with various techniques including density-functional theory (DFT), molecular mechanics (MM), and Monte Carlo (MC) simulation based on an interaction-site model. The second-generation asymmetric Fréchet dendrons consist of three phenyl rings, two of which are functionalized by two pairs of alkoxy chains, a longer dodecyloxy pair, and a shorter octyloxy pair (see Fig. 1 left), responsible for van der Waals and weak hydrogen bonds.[22] The fact, that Fréchet dendrons with longer and shorter chains are used, eases identification of angles within conformers. Otherwise, the irregular chain length is of no importance, as a large pattern variety is also obtained for chain-symmetric Fréchet dendrons (two pairs of octyloxy chains), see Ref. 15. The total van der Waals interactions are the sum of the individual intermolecular interactions [chain-neighboring-chain (c-n-c)] and the molecule-substrate interactions [molecule-substrate (m-s)]. By varying the internal angles of the pairs of alkoxy chains in an interaction-site model, all facets of the experimentally found patterns can be predicted within our approach. A zero-temperature analysis of the MC simulations leads to the thermodynamically most stable pattern that corresponds both to the local minimum derived from MM simulations and the experimental findings upon heating the monolayers.

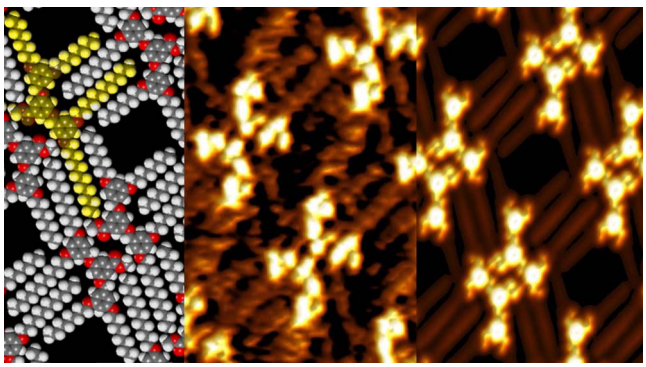

FIG. 1. (Color online) A single molecule of the dodecyl/octyl terminated Fréchet dendron is highlighted. One of seven different ordering patterns on HOPG is exemplified. *Middle*: STM image of a jigsaw pattern of the Fréchet dendron (7.5 nm × 12.5 nm, U_{Bias}=−800 mV, $|I_T|$=8 pA). *Left*: atomistic modeling by an energy minimized MM simulation (see text). *Right*: simulation of the LDOS by DFT calculations based on the input of the geometry determined by MM.

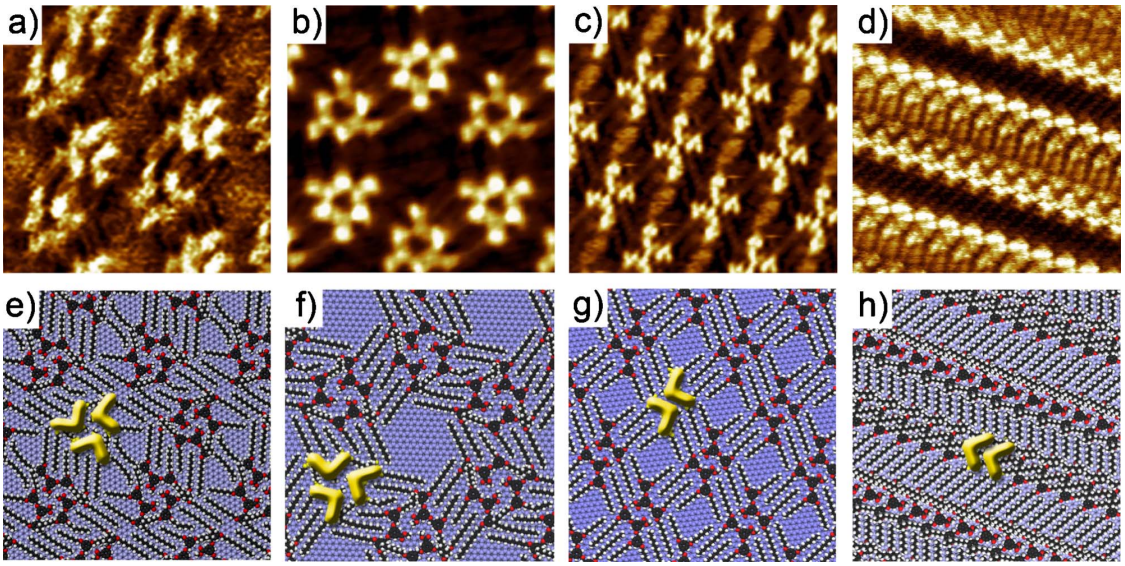

FIG. 2. (Color online) [(a)–(d)] STM results and corresponding [(e)–(f)] molecular mechanics modeling (see text) of four experimentally found patterns of Fréchet dendrons: (a) sawtooth, (b) honeycomb, (c) jigsaw, and (d) tiretrack. The molecular backbones (highlighted) indicate the local ordering motif. (10 nm × 10 nm, $U_{Bias}=-700$ to -800 mV, and $|I_T|=5-30$ pA)

II. METHODS

For the STM measurements a nanoscope multimode III instrument equipped with a low-current converter under ambient conditions was employed. Monolayers of Fréchet dendrons (3,5-bis[(3,5-bisoctyloxyphenyl)methyloxy]phenyl ester, synthesis, see Ref. 23), are cast from 0.2 mM solutions in ethanol, hexane, or heptadecane on highly oriented pyrolytic graphite (HOPG) surfaces. The emerging patterns are analyzed by combining several complementary approaches: (a) DFT, utilizing the CASTEP®module of Material Studio 4.3 employing Perdew-Wang'91 generalized gradient approximation exchange correlation functionals[24] and a plane-wave-basis set with an energy cutoff at 260 eV; (b) MM, performed on a fixed double layer of graphite (universal force fields[25] in periodic boundary conditions) based on starting values obtained from the STM experiments; and (c) MC annealing simulations in the METROPOLIS scheme based on 60° rotations of a coarse-grained interaction-site model, using periodic boundary conditions for minimizing finite-size effects in system sizes ranging from several hundreds to a few thousand objects.

III. RESULTS AND ANALYSIS

The mixed image in Fig. 1 (Ref. 26) exemplifies MM and DFT simulations together with experimental measurements of the jigsaw pattern. After applying a droplet of a solution in hexane, the jigsaw pattern ($p2$ symmetry)[27] appears as one of seven general ordering motifs in about 25% of the substrate area. A detailed analysis of many STM images yields starting configurations[28] for a MM energy minimization[29] to calculate molecular conformations (see left of Fig. 1) and relative positions. From the MM determined adsorption energy the dominant van der Waals part[30] can be extracted, as discussed later.

As the energy-minimized MM simulations can only provide atomic positions and not electronic states, we used these energy minimized geometries as input to derive the local density of states (LDOS) of a free single molecule using DFT. Convoluted[31] density contours of a planar slice in the LDOS are plotted[32] (right, Fig. 1) for a direct comparison with the STM measurement: the phenyl rings of the molecular cores are discernible as three bright protrusions and atoms of the alkoxy arms emerge (visible in the dark areas) as series of faint lines (right, Fig. 1) in agreement with the experimental STM images (middle, Fig. 1).

In a large STM study, we have imaged seven ordering motifs of this Fréchet dendron in excellent resolution. Here we focus on four main ordering motifs: sawtooth: honeycomb: jigsaw: tiretrack (see Fig. 2). 20 nm × 20 nm sized domains of these patterns in ratios 1%:15%:25%:20% typically cover an HOPG surface roughly half an hour after applying a hexane droplet. About 39% of the HOPG surface is occupied by domain boundaries, mobile molecules or two other patterns: upright and small tiretrack. Minutes after casting a droplet of the Fréchet dendrons in hexane, the honeycomb pattern dominates. The sawtooth pattern seldom appears as an independent pattern and often as a stacking fault of the honeycomb pattern. After several hours, typically 60% of the HOPG surface is covered with the tiretrack pattern.

As DFT calculations can only poorly describe van der Waals interactions, the dominant part of the internal energy, the adsorption energy per unit cell or area, is evaluated from the MM minimization energy.[33] This covers the dominant intermolecular interactions stemming from the alkoxy chains, statistically contributing an interaction strength of 14 kJ/mol per four CH_2 units in case of alkoxy chains that are not fully (>50%) interdigitated on graphite (previous studies yield 18 kJ/mol for fully and 8.5 kJ/mol for half-interdigitated alkoxy chains on graphite surfaces[34]). We have calculated the van der Waals part of the total energy (I) of a

TABLE I. Van der Waals part of the adsorption energies determined by MM energy minimization. (a) *per molecule*. (b) *per area*. The labels refer to: m-s, molecule-substrate interactions and c-n-c, chain-neighboring-chain interactions.

Pattern	Molecules per unit cell	$I_{\text{m-s}}$/molecule (kJ/mol)	$I_{\text{c-n-c}}$/molecule (kJ/mol)
Sawtooth	6	−674	−147
Honeycomb	6	−691	−163
Jigsaw	2	−653	−117
Tiretrack	2	−528	−222

Pattern	Unit cell size (nm^2)	$I_{\text{m-s}}/nm^2$ (kJ/mol)	$I_{\text{c-n-c}}/nm^2$ (kJ/mol)
Sawtooth	24.5	−167	−38
Honeycomb	26.5	−155	−38
Jigsaw	8.4	−151	−25
Tiretrack	6.1	−172	−75

substrate supported monolayer in MM energy minimized geometry, i_{sup}, (II) of a gas phase net,[2] i_{gn}, and (III) of one isolated molecule, i_{iso}. With that we can carefully separate the intermolecular interaction (chain-neighboring-chain) part $I_{\text{c-n-c}}/\text{molecule}=(i_{gn}/n)-i_{iso}$ from the substrate interaction (molecule-substrate) part $I_{\text{m-s}}/\text{molecule}=(i_{gn}-i_{sup})/n$ of the van der Waals energy per molecule, with n, the number of molecules per unit cell (see Table I). If we then divide by the area per unit cell, the respective energies per nm^2 are derived (see Table I).

Molecular domains grow at the boundaries by the addition or loss of molecules that do not have a full complement of neighboring molecules as appropriate for the domain symmetry. When initially forming domains after applying a droplet, the gain in van der Waals adsorption energy $I_{\text{m-s}}+\delta(I_{\text{c-n-c}})$ *per molecule* with $\delta<1$ rules the process: the honeycomb pattern in Table I. Over time the HOPG surface is covered with some 100-nm^2-sized domains, which transform according to the Kitaigorodskii principle of avoiding free space.[35] Hence the highest gain in van der Waals adsorption energy $I_{\text{m-s}}+I_{\text{c-n-c}}$ *per area* dominates the outcome: the tiretrack pattern in Table I. This agrees with the thermodynamically stable pattern experimentally identified by moderate heating, which is the tiretrack pattern in hexane. Thus, the initial domains form open pore patterns dominated by the highest energy gain *per molecule* while with time the pattern with the largest energy gain *per area* wins. However, all calculated energies are very close, reflecting that the phases can coexist.

IV. MODELING

In order to identify the ground-state energy we performed independent MC simulations, based on coarse graining the dominant molecule and substrate properties in an interaction-site model. Rather than including as much chemical detail as possible, we investigated the crucial properties needed to reproduce key experimental findings. When large molecules adsorb on ten or more substrate atoms, the organization is dominated by steric hindrance; the role of the substrate is to align the molecular backbone and to some extent the molecular chains. In this work, we systematically varied the internal angles of the pairs of longer and shorter arms of interaction centers (see Fig. 3), thereby probing different molecular conformations, in order to determine how critical the angles are on the predictive power of the interaction-site model.

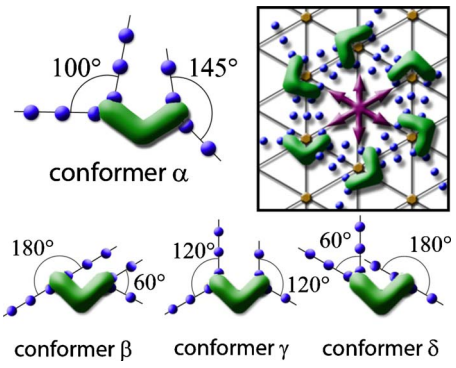

FIG. 3. (Color online) Top: angle configuration for conformer α. The box displays the six possible orientations on a fixed lattice of hexagonal symmetry. Bottom: conformers β, γ, and δ with the respective internal angles indicated.

As described in our previous work[15] the substrate symmetry is accounted for by allowing discrete $\pi/3$ rotations of the coarse grained molecules, see Fig. 3, on fixed sites in a lattice of hexagonal symmetry. The geometry and spacing of the molecular backbone is transferred from the MM modeling. The chains are modeled by a small number of beads, disposed in rigid, straight arms at distances determined by MM and with approximate angles of 100° and 145° between long and short pairs of alkoxy chains, respectively.[15] We refer to a Fréchet dendron with the latter chain conformation as conformer $\boldsymbol{\alpha}$. Here, the internal angle within each pair of arms has been systematically varied from 180° and 60°, referred to as conformer β, over 120° and 120°, conformer γ, to 60° and 180°, conformer δ, for long and short pairs of alkoxy chains, respectively. One bead represents four CH_2 units, exhibiting short-range van der Waals attractions, which are described by a Lennard-Jones potential, $U(r)=4\epsilon[(\sigma/r)^{12}-(\sigma/r)^6]$.

The MC simulations were performed by preparing random starting configurations [see (0) in Fig. 4] and relaxing the system by slowly "cooling." The lattice constant a, accounting for the density, has been varied between 2.95σ and 4.0σ, corresponding to a change in coverage density by a factor of 1.35, while the dimensionless inverse temperature ϵ/k_BT ranged from 0.025 to 6. The ordered patterns obtained, (i), (ii), (iii), and (iv) in Fig. 4, correspond well in long-range symmetry and local ordering with the structures found experimentally: (a), (b), (c), and (d) in Fig. 2, respectively. While the chain configuration of conformer α (100° and 145° for long and short pairs of alkoxy chains, respectively) leads to a striking variety of patterns (see Ref. 15), the systematic choice of internal angles in conformers β, δ, and γ narrows the pattern variety.

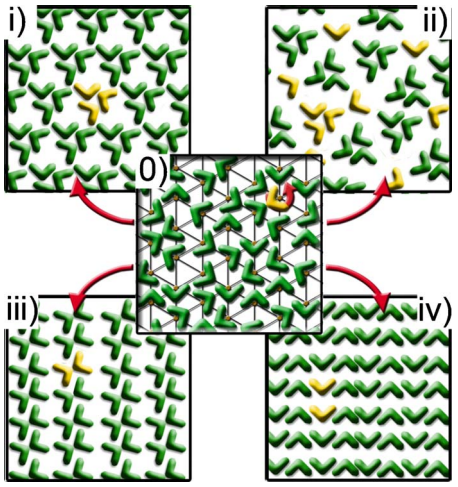

FIG. 4. (Color online) MC simulations (i)–(iv). (0) Random starting configurations allowing discrete $\pi/3$ rotations of the coarse grained molecules. Upon slow cooling the following patterns formed from random state (0) indicated with red arrows: (i) sawtooth pattern for conformer β and for conformer α, (ii) trimer honeycomb pattern for conformer δ, (iii) jigsaw pattern for conformer α, and (iv) tiretrack pattern for conformers α, β, and γ. All phases were stable upon heating to 300 °C.

The patterns that can be generated from the respective conformers are: sawtooth and tiretrack for β [see (i) and (iv) in Fig. 4], tiretrack, honeycomb, and inverted honeycomb for γ [see (iv) in Fig. 4 and (v) and (vi) in Fig. 5, respectively] and trimer honeycomb for δ [see (ii) in Fig. 4]. So with the conformer δ, even the intriguing open-pore host structure of the molecular trimers arranged in hexagonal symmetry [see (b) in Fig. 2] can now be generated from random starting configurations by slow cooling. The honeycomb pattern (b) in Fig. 2 displays an organizational chirality with an included guest molecule of nonfixed orientation (described in another publication[36]). Hence, all experimentally found patterns can be completely described. The MC patterns (i)–(iv), in very good correspondence with experimental findings, proved to be reliable, as raising the temperature showed that these phases stay ordered up to 300 °C and can thus be considered as stable states.

Furthermore, we now demonstrate two additional patterns (see Fig. 5) named (v) honeycomb pattern and (vi) inverted honeycomb pattern (both found for conformer γ), that were condensed from random starting configurations, but could not be verified in the STM experiments. The stability of these MC patterns was tested by simulating a finite temperature; both patterns proved unstable upon "heating" and, thus, cannot be considered likely ordering states. Although, all three honeycomb patterns have a similar appearance, upon closer examination, only the trimer honeycomb pattern (ii) displayed in Fig. 4 correctly describes the experimentally found pattern (b) of Fig. 2. Hence, the honeycomb and inverted honeycomb pattern are not experimentally observed and are unstable in a MC simulation of finite temperature.

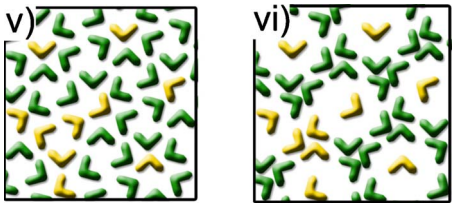

FIG. 5. (Color online) Alternative phases, that have been predicted, condensed from random starting configurations by the Monte Carlo approach: (v) honeycomb pattern of conformer α and γ, and (vi) inverted honeycomb pattern of conformer γ. Both the inverted honeycomb and honeycomb MC patterns proved unstable upon simulating a finite temperature and, thus, cannot be considered as likely patterns; these patterns find no close resemblance in the experimental data.

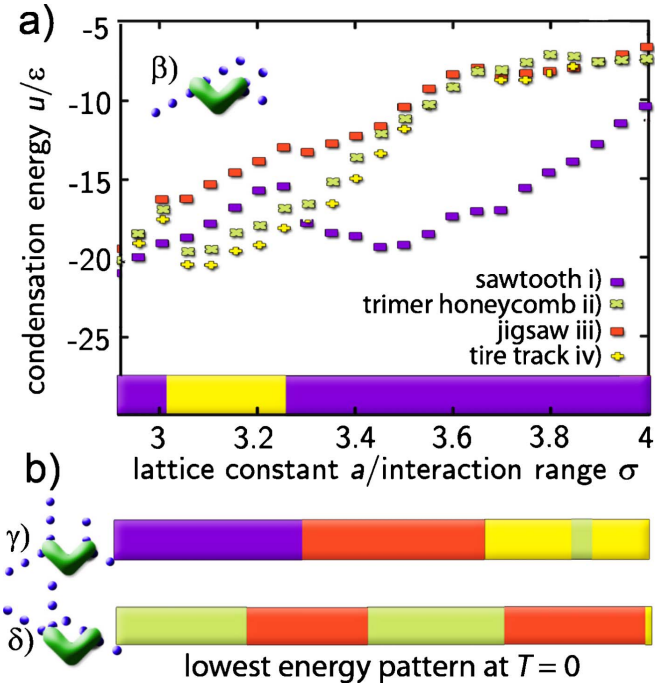

FIG. 6. (Color online) conformer β, coarse grained model with angles 180° and 60° between the long and short chains. (a) Zero-temperature energy analysis for determining the associated lowest energy state. The experimentally relevant regime corresponds to $3.2a/\sigma$. (b) The pattern of lowest energy in the zero-temperature analysis for conformations γ and δ. At the experimentally relevant regime of $3.2a/\sigma$, the sawtooth pattern for conformer γ and jigsaw pattern for conformer δ, did not prove stable upon heating and hence cannot represent the thermodynamically most stable pattern.

In contrast to patterns generated from random starting configurations, patterns (i), (ii), (iii), and (iv) (see Fig. 4) can be pre-prepared for all conformers allowing to compute the associated energies in a zero-temperature energy analysis. So the state of lowest energy at $T=0$ can be identified in each case as a function of the packing density. In the case of artificially prepared patterns the energy analysis can only indicate how energetically attractive a structure is, not if the pattern is likely. The pattern that minimizes the energy varies, depending on the packing fraction [see bar graphs in Figs. 6(a) and 6(b)] and the internal angle, hence, the conformer. In the experimentally relevant regime ($3.2a/\sigma$), the most favorable configuration for conformer α (see Ref. 15) and conformer β) is the tiretrack pattern [see Fig. 6(a)]. As this pre-prepared pattern is stable upon heating to 300 °C

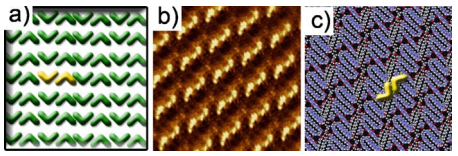

FIG. 7. (Color online) (a) Another local ordering motif of the MC simulation [Fig. 4(iv)] that was subsequently identified experimentally; (b) STM measurement of the rarely found fifth pattern with corresponding; and (c) MM modeling. (12.5 nm × 12.5 nm, U_{Bias}=−800 mV, $|I_T|$=8 pA)

and can also be generated from random starting configurations, the tiretrack pattern is identified as the thermodynamically most stable pattern in good agreement with the experimental findings and the MM energy analysis discussed above.

For the chain configurations of conformers γ and δ, the sawtooth and jigsaw patterns [Fig. 6(b)] appear to have the lowest energy at T=0 in the experimentally relevant regime. Probing the stability of the latter two patterns by raising the temperature leads to destabilization and, thus, clearly indicates that neither the sawtooth nor jigsaw can represent the thermodynamically most stable pattern around room temperature.

In summary, the systematic variation in internal angles within the pairs of chains (representing the chain-chain interdigitation) reveals that the local and global ordering motif of all experimentally found patterns can be reproduced by cooling random starting configurations. The zero-temperature analysis of pre-prepared patterns in all combinations of conformers/patterns underlines that only the tiretrack pattern found for conformer α (see Ref. 15) and β represents an ordered state with lowest energy at T=0 and is at the same time stable upon heating. Thus, the tiretrack pattern is confirmed both experimentally and theoretically as the thermodynamically most stable motif at finite temperatures, even for different molecular conformations in the interaction-site model.

In addition, it is not only possible to reproduce patterns by the MC approach but also to predict. In Fig. 4(iv) a second local ordering motif with a side by side arrangement of the molecular backbones is apparent [Fig. 7(a)]. This local ordering motif named "wave" has been experimentally identified subsequent to the theoretical prediction; it occurs rarely for dodecyl/octyl terminated Fréchet dendrons in ethanol [Fig. 7(b)].

V. CONCLUSIONS

Our study underlines the assertion that gross geometrical features are the dominant driving force of molecular self-organization. The various patterns found experimentally for the Fréchet dendron presented in this study serve as a versatile model system to systematically test our multimodeling approach. Five structural phases have been closely modeled by MM energy minimization; their quality is underlined in an exemplary manner by DFT LDOS simulations plotted adjacent to the STM image. Evaluating the van der Waals part of the MM determined adsorption energy favors an open pore trimer honeycomb structure in the initial phase of adsorption (energy per molecule maximized) and a densely packed pattern reminiscent of tire tracks after various phase transformations to reach the final state (energy per area maximized). The calculated energies are very similar reflecting the coexistence of phases for competing ordering motifs. Furthermore, we have refined our independent MC approach with a coarse grained interaction-site model of various internal angles and can successfully reproduce the experimental pattern diversity in all facets of the local and global ordering. The lowest energy pattern at T=0 can be identified in a zero-temperature analysis for the different chain conformations. All theoretical and experimental findings point to the tiretrack pattern as the thermodynamically most stable pattern for the dodecyl/octyl terminated Fréchet dendron. Furthermore, a newly predicted local ordering motif has been experimentally verified subsequently. We thoroughly and successfully tested an interaction-site approach to molecular self-organization, which will serve as an innovative analysis tool in the future fostering the application of self-organized molecular monolayers in various areas of science.

ACKNOWLEDGMENTS

Financial support by the German Excellence Initiative via the program "Nanosystems Initiative Munich (NIM)," ERA-Chemistry, Studienstiftung des dt. Volkes, IDK NanoBio-Technology, CeNS, NRP47, and the Swiss Nanoscience Institute is gratefully acknowledged. We thank K. Gruber for participating in the development of the interaction-site model and E. Constable for important chemical input to the latter model, C. Höhl for measuring the wave pattern with STM, L. Merz, M. Malarek, and L. Scherer for prior STM measurements on Fréchet-dendrons, L. Scherer and F. Trixler for discussing symmetries of patterns, D. Amann, L. Merz, and I. Widmer for finding measurement protocols, E. Constable, S. Graber, C. Housecroft, M. Malarek, P. B. Rheiner, D. Seebach, and L. Scherer for synthesis of compounds, M. Schönherr for input on MM energy optimization, P. Altpeter, H. Lorenz, and S. Schöffberger for support in the clean room, R. Gross, H. J. Güntherodt, J. Kotthaus, J. Rädler, and F. Simmel for usage of facilities and ongoing support. F. Jamitzky, R. Netz, P. Nielaba, S. Rohr, and A. Rubio are acknowledged for discussions.

*Author to whom correspondence should be addressed; b.hermann@cens.de

[1] G. Pawin, K. L. Wong, K. Y. Kwon, and L. Bartels, Science **313**, 961 (2006).
[2] J. Schnadt, E. Rauls, W. Xu, R. T. Vang, J. Knudsen, E. Lægsgaard, Z. Li, B. Hammer, and F. Besenbacher, Phys. Rev. Lett. **100**, 046103 (2008).
[3] A. Langner, S. L. Tait, N. Lin, C. Rajadurai, M. Ruben, and K. Kern, Proc. Natl. Acad. Sci. U.S.A. **104**, 17927 (2007).
[4] K. Tahara, S. Furukawa, H. Uji-i, T. Uchino, T. Ichikawa, J. Zhang, W. Mamdouh, M. Sonoda, F. C. De Schryver, S. De Feyter, and Y. Tobe, J. Am. Chem. Soc. **128**, 16613 (2006).
[5] J. V. Barth, Annu. Rev. Phys. Chem. **58**, 375 (2007).
[6] G. Tomba, L. C. Ciacchi, and A. De Vita, Adv. Mater. **21**, 1055 (2009).
[7] B. Ilan, G. M. Florio, M. S. Hybertsen, B. J. Berne, and G. W. Flynn, Nano Lett. **8**, 3160 (2008).
[8] D. X. Shi, W. Ji, X. Lin, X. B. He, J. C. Lian, L. Gao, J. M. Cai, H. Lin, S. X. Du, F. Lin, C. Seidel, L. F. Chi, W. A. Hofer, H. Fuchs, and H. J. Gao, Phys. Rev. Lett. **96**, 226101 (2006).
[9] J. V. Barth, G. Costantini, and K. Kern, Nature (London) **437**, 671 (2005).
[10] J.-M. Lehn, Science **295**, 2400 (2002).
[11] M. Ortega Lorenzo, C. J. Baddeley, C. Muryn, and R. Raval, Nature (London) **404**, 376 (2000).
[12] C. Joachim, J. K. Gimzewski, and A. Aviram, Nature (London) **408**, 541 (2000).
[13] K. Morgenstern, S. W. Hla, and K. H. Rieder, Surf. Sci. **523**, 141 (2003).
[14] C. Meier, U. Ziener, K. Landfester, and P. Weihrich, J. Phys. Chem. B **109**, 21015 (2005).
[15] C. Rohr, M. Balbás Gambra, K. Gruber, E. C. Constable, E. Frey, T. Franosch, and B. A. Hermann, Nano Lett. **10**, 833 (2010).
[16] A. Breitruck, H. E. Hoster, and R. J. Behm, J. Phys. Chem. C **113**, 21265 (2009).
[17] U. K. Weber, V. M. Burlakov, L. M. A. Perdigao, R. H. J. Fawcett, P. H. Beton, N. R. Champness, J. H. Jefferson, G. A. D. Briggs, and D. G. Pettifor, Phys. Rev. Lett. **100**, 156101 (2008).
[18] M. Haran, J. E. Goose, N. P. Clote, and P. Clancy, Langmuir **23**, 4897 (2007).
[19] A. Šarlah, E. Frey, and T. Franosch, Phys. Rev. Lett. **95**, 088302 (2005); Phys. Rev. E **75**, 021402 (2007).
[20] C. J. Hawker and J. M. J. Fréchet, J. Am. Chem. Soc. **112**, 7638 (1990); J. Chem. Soc., Chem. Commun. **1990**, 1010.
[21] B. A. Hermann, L. J. Scherer, C. E. Housecroft, and E. C. Constable, Adv. Funct. Mater. **16**, 221 (2006).
[22] Omitted due to a much smaller contribution.
[23] E. Constable, S. Graber, B. A. Hermann, C. E. Housecroft, M. S. Malarek, and L. J. Scherer, Eur. J. Org. Chem. **2008**, 2644 (2008).
[24] S. J. Clark, M. D. Segall, C. J. Pickard, P. J. Hasnip, M. I. J. Probert, K. Refson, and M. C. Payne, Z. Kristallogr. **220**, 567 (2005).
[25] A. K. Rappé, C. J. Casewit, K. S. Colwell, W. A. Goddard III, and W. M. Skiff, J. Am. Chem. Soc. **114**, 10024 (1992).
[26] Images flattened, correlation averaged, and drift-corrected.
[27] E. C. Constable, M. Haeusler, B. A. Hermann, C. E. Housecroft, M. Neuburger, S. Schaffner, and L. J. Scherer, Cryst. Eng. Comm. **9**, 176 (2007).
[28] Starting with an energy-minimized free molecule has failed at 150% minimization energies.
[29] Unit cell of two molecules in periodic boundary conditions.
[30] Electrostatic interactions contribute only 30%.
[31] With a Gaussian function of 2× a Pt d_z orbital, 200 pm.
[32] Eight free molecules at precisely MM-determined positions.
[33] Omitting electrostatic interactions.
[34] S. Yin, C. Wang, X. Qiu, B. Xu, and C. Bai, Surf. Interface Anal. **32**, 248 (2001).
[35] A. I. Kitaigrorodskii, C. Wang, X. Qiu, B. Xu, and C. Bai, *Molecular Crystals and Molecules* (Academic Press, New York, 1973).
[36] L. Merz, H.-J. Güntherodt, L. J. Scherer, E. C. Constable, C. E. Housecroft, M. Neuburger, and B. A. Hermann, Chem.-Eur. J. **11**, 2307 (2005).